

Layer-by-layer assembled dual-ligand conductive MOF nano-films with modulated chemiresistive sensitivity and selectivity

Ai-Qian Wu¹, Wen-Qing Wang¹, Hong-Bin Zhan¹, Lin-An Cao², Xiao-Liang Ye², Jia-Jia Zheng³, Pendyala Naresh Kumar², Kashi Chiranjeevulu², Wei-Hua Deng², Guan-E Wang², Ming-Shui Yao^{2,3} (), and Gang Xu² ()

© Tsinghua University Press and Springer-Verlag GmbH Germany, part of Springer Nature 2020 **Received:** 20 February 2020 / **Revised:** 7 April 2020 / **Accepted:** 19 April 2020

ABSTRACT

In this paper, a dual-ligand design strategy is demonstrated to modulate the performance of the electronically conductive metalorganic frameworks (EC-MOFs) thin film with a spray layer-by-layer assembly method. The thin film not only can be precisely prepared in nanometer scale (20–70 nm), but also shows the pin-hole-free smooth surface. The high quality nano-film of 2,3,6,7,10,11-hexaiminotriphenylene (HITP) doped Cu-HHTP enables the precise modulation of the chemiresistive sensitivity and selectivity. Selectivity improvement over 220% were realized for benzene vs. NH₃, as well as enhanced response and recovery properties. In addition, the selectivity of the EC-MOF thin film sensors toward other gases (e.g. triethylamine, methane, ethylbenzene, hydrogen, butanone, and acetone) vs. NH₃ at room temperature is also discussed.

KEYWORDS

metal-organic frameworks, electronic conductivity, dual-ligand, thin films, gas sensors

1 Introduction

Electronically conductive metal-organic frameworks (EC-MOFs) are a newly emerging type of porous conductive material constructed by the periodic connection of metal ions and redox-active organic units [1-5]. EC-MOFs possess crystalline state, narrowly distributed size and regularly arranged pores, the tunable band gap, as well as the designable charge transport pathway [6-14]. The unique combination of porosity and conductivity enables them to answer the question whether EC-MOFs can be applied to electrical applications. Together with the boosting researches on doped EC-MOFs or EC-MOF based composites, EC-MOFs as promising materials for electrical applications have been proofed by excellent cases including electrocatalysis [15], supercapacitors [16-18], chemiresistive gas sensors [3, 19-23], field effect transistors (FETs) [24], photo-catalysis [25, 26], and lithium-sulfur battery [27]. While semiconducting two-dimensional (2D) π-conjugated EC-MOFs showed exciting properties as active materials with satisfactory stability [3, 6, 28], state of the art 2D π -conjugated EC-MOF semiconductors mainly focus on single redox-active ligand systems with mono-/bi-metallic nodes [3, 28, 29]. Meanwhile, the effects of the dual-ligand with dissimilar functional motifs on the semiconducting behaviors of the 2D π -conjugated EC-MOF thin film have not been reported yet.

Considering the inherent simpleness in concept (resistance change), chemiresistive gas sensors are the simplest and most widely applied semiconductor devices among various gas sensors

[30–35]. In terms of long-term bottlenecks of poor selectivity and high operating temperature, EC-MOFs are utilized as active sensing materials in consideration of their high porosity, specific guest-framework interaction and room temperature (RT) activity [13, 20, 31, 36-38], which can potentially cope with the issue. However, the detecting gases of the pristine EC-MOF chemiresistor are limited to strong reducing/oxidizing molecules such as NO₂, NH₃, H₂S, and NO, which hinders the extensive applications of such new generations of RT gas sensors. To broaden window of detectable gases by either improvements on quality of the film or introduction of a secondary MOF capable of gas separation [39, 40], both sensitivity and selectivity were enhanced by the fabrication of EC-MOF nano-film [20], and MOF-on-MOF thin films [41-43], respectively. Even so, continuous modulation of both sensitivity and selectivity by a single type of EC-MOF chemiresistor is still challenging.

Here, we propose a novel dual-ligand design strategy to modulate the performance of EC-MOF thin film chemiresistor by a spray layer-by-layer (LbL) liquid-phase epitaxial growth method. In this regard, two redox-active ligands with different coordination groups, namely 2,3,6,7,10,11-hexahydrotriphenylene (HHTP, –OH) and 2,3,6,7,10,11-hexaiminotriphenylene (HITP, –NH₂), were utilized to prepare the hexagonal HITP doped Cu-HHTP-10C nanofilm (Fig. 1). The similar crystal structure of their pristine frameworks (Cu₃(HHTP)₂ and Cu₃(HITP)₂) enabled the successful synthesis of dual-ligand EC-MOFs. Since the hybrid framework significantly altered the electronic structure, the chemiresistive sensing performances are thus

¹ College of Materials Science and Engineering, Fuzhou University, Fuzhou 350108, China

² State Key Laboratory of Structural Chemistry, Fujian Institute of Research on the Structure of Matter, Chinese Academy of Sciences, Fuzhou 350002, China

³ Institute for Integrated Cell-Material Sciences (WPI-iCeMS), Kyoto University Institute for Advanced Study, Kyoto University, Yoshida Ushinomiya-cho, Sakyo-ku, Kyoto 606-8501, Japan

Nano Res.

modulated. The thin film not only can be precisely prepared in nanometer scale (20-70 nm), but also shows the pin-hole-free smooth surface. By this manner, the sensitivity and selectivity of the HITP doped Cu-HHTP-10C nanofilm toward different reducing gases can be well controlled. Moreover, enhanced sensing response and recovery properties were also realized by proper doping of HITP into Cu₃(HHTP)₂ frameworks.

Results and discussion

Both Cu₃(HHTP)₂ and Cu₃(HITP)₂ shows a honeycomb-like porous crystal structure with a 2D hexagonal layer of Cu-ligand in the ab plane, and a slipped-parallel AB stacking model with an interval distance of 3.3 Å along the c-axis (Fig. 1). Rich polar organic functional groups and open Cu sites are located on the one-dimensional (1D) channel with a diameter of ~ 1.8 nm. The -OH functionalized substrates (e.g. sapphire, Si/SiO₂, and quartz) were used to facilitate the growth of the dual-ligand EC-MOF thin film (Fig. 1). After alternative exposure to the ethanolic solution of copper(II) acetate (0.1 mM) and the mixed ethanolic solution of dual-ligands with 10 cycles, the HITP doped Cu-HHTP-10C with different doping percentages can be obtained (Fig. 1, details see the Electronic Supplementary Material (ESM)). The mixed dual-ligands solution was obtained by mixing different molar ratio of HHTP (0.01 mM) and HITP (0.1 mM, the pH value was 8.5 regulated by ammonium hydroxide (28%)). After every spray, the substrate was kept steady for 20 s to ensure the growth of the HITP doped Cu-HHTP-10C thin film. Between each spray step, the substrate was rinsed with absolute ethanol to remove the residual reactants to ensure the controlled growth in the nanometer scale. To completely remove residual organic ligands or solvents, HITP doped Cu-HHTP-10C thin films were activated by successive immersions in N,Ndimethyl formamide (DMF) and ethanol at RT.

Figure 2(a) and Figs. S1-S5 in the ESM show the atomic force microscopy (AFM) images of the typical top and edge view of the HITP doped Cu-HHTP-10C nano films. All the thin films are pinhole-free, dense and continuous, which can also be confirmed by scanning electron microscopy (SEM) measurements (Fig. S6 in the ESM). The HITP doping effects on the thickness and roughness of the thin film are summarized in Fig. 2(b). Compared with pristine Cu₃(HHTP)₂-10C thin film, the thickness gradually increased with increasing HITP dopants, while the calculated root mean square (RMS) surface roughness shows slight change for low HITP dopants but increases sharply when the dopant is higher than 5.0 mol%. As

mentioned above, the mixed ethanolic solution of dual ligands contains ammonium hydroxide used for the pH value regulation of HITP. In our previous work, the thickness increments of Cu-HITP and Cu-HHTP are similar to each other (~ 2 nm per cycle). In contrast, the AFM results clearly reveal the enhanced growth of dual-ligand Cu-HHTP/HITP thin film by ammonium hydroxide, especially in high concentration cases. The possible reason might lie in the remarkable growth of Cu-HHTP owing to pH change of dual-ligand solutions. Even so, the thickness and roughness of all the HITP doped Cu-HHTP-10C nano films can be controlled to less than 80 and 15 nm, respectively. The dual ligand doping process can be further confirmed by monitoring HITP doped Cu-HHTP-10C nano films on the quartz substrate with the UV-Vis spectrum. As shown in Fig. S7 in the ESM, the intensity increments of the maximum absorption peaks for Cu-HITP (212 nm) and Cu-HHTP (353 nm) differ from each other. Accordingly, the value of I212nm/I353nm for the 5.0 mol% sample is higher than the 0.5 mol% sample because of the contribution of higher HITP dopants.

For the sample with high resistance (> 1,000 Ω), the two-probe method is normally adopted for electrical measurements. For HITP dopants lower than 1.0 mol%, the value of conductivity (defined as σ/C_0 here, details see the ESM) is notably increased ~ 2 orders of magnitude due to the formation of highly conductive coordination of Cu ions with o-phenylenediamine linkages via the successful doping (Fig. 2(c)) [13, 21]. Nonetheless, for HITP dopants higher than 1.0 mol%, the σ/C₀ showed slight change due to negative effects of the reduced quality of thin films. The success doping of HITP can be further confirmed by X-ray photoelectron spectroscopy (XPS) spectra with typical peaks of Cu, C, O and N (Fig. 2(d)). As a surface-sensitive semi-quantitative spectroscopic technique, high resolution O1s and N1s peaks indicate that the ratio of HITP to HHTP of the thin films increased with the increasing molar ratio of HITP and HHTP in the mixed dual-ligand solution (Fig. 2(e)). For the thin film using high molar ratio of HITP (1.0 mol% or higher), significant peaks of non-lattice oxygen (vacancy O_v, chemisorbed or dissociated OH species O_{OH}) were observed. This may possibly owe to the competitive coordination of two different ligands with Cu ions, which gives rise to framework defects like missing Cu nodes, free -OH groups of HHTP, etc.

As active materials of chemiresistive gas sensors reported in recent years, pristine Cu-HHTP is a p-type semiconductive MOF material with a conductivity of ~ 0.02 S·cm⁻¹ at RT (pellet, 2 probes) [44], while pristine Cu-HITP is a n-/p-type

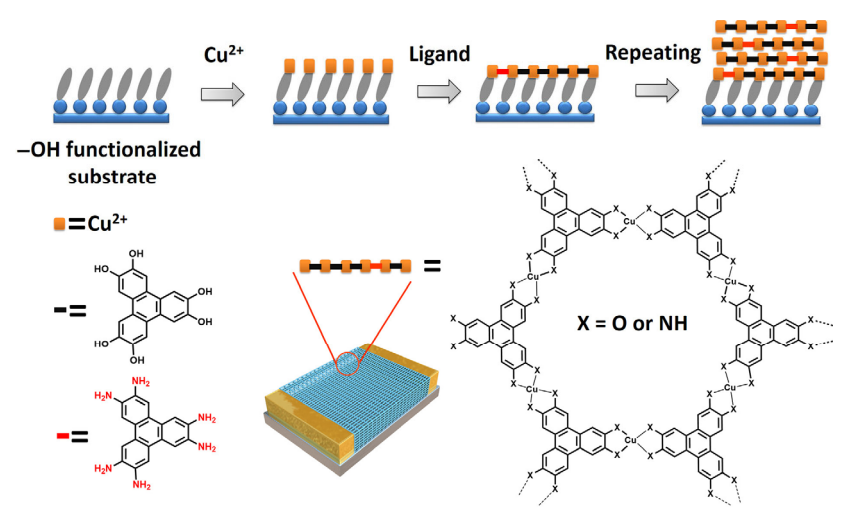


Figure 1 Schematic illustration of the preparation of HITP ligand doped Cu-HHTP-10C thin film gas sensors.

Nano Res. 3

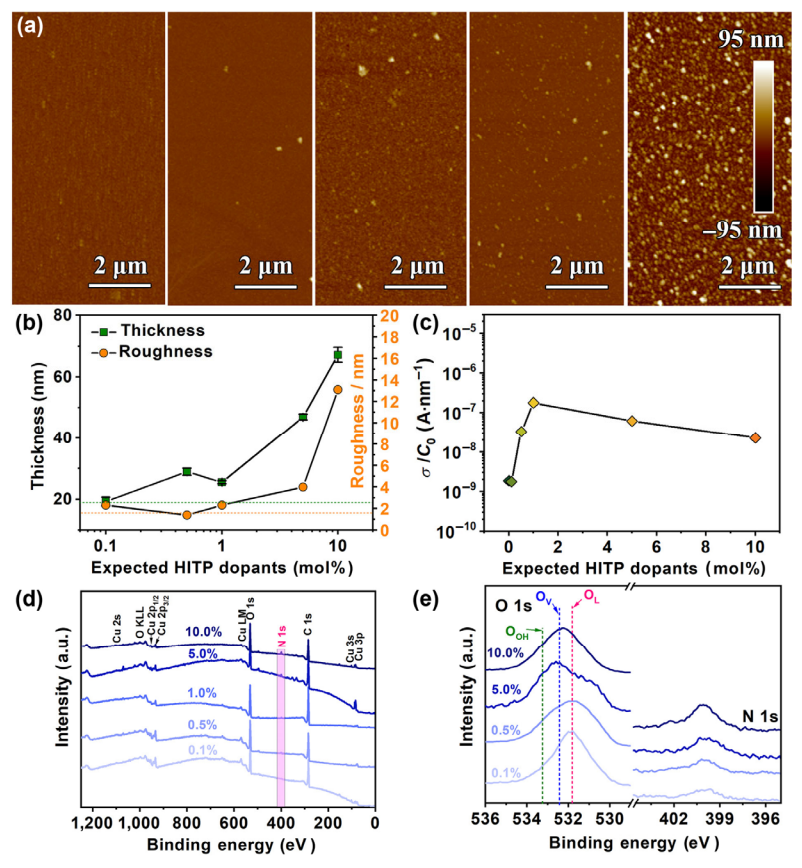


Figure 2 Top views of HITP doped Cu-HHTP-10C: (a) AFM image (from left to right, HITP mol%, 0.1, 0.5, 1.0, 5.0, and 10.0), (b) HITP dopant dependent thickness and roughness, (c) HITP dependent thin film current divided by their thickness to represent conductivity (σ/C_0 , C_0 is a constant for a given interdigital electrodes and voltage), (d) XPS spectra and (e) high resolution XPS spectra at binding energies corresponding to O 1s and N 1s, respectively.

(depends on defects formed during synthesis) semiconductive MOF material with a conductivity of $\sim 0.2~{\rm S\cdot cm^{-1}}$ at RT (pellet, 2 probes) [21]. The combination of two ligands with different redox activity enables the modulation of electronic structure due to differences in the contribution to highest occupied molecular orbital (HOMO) levels, defect-related energy levels, etc. Therefore, the activated HITP doped Cu-HHTP-10C nano films on sapphire substrates precoated with interdigital Au electrodes were directly used as the chemiresistors for the detection of 8 different reducing gases (for details, see the ESM).

Figure 3(a) shows the typical response-recovery curve of HITP doped Cu-HHTP-10C to benzene gas of different concentrations (1–100 ppm). All sensors exhibited the increased resistance upon exposure toward benzene gas, which is the typical behaviour of a p-type semiconductor and consistent with the pristine Cu-HHTP. Interestingly, the normalized current curves present good response-recovery to 100 ppm of benzene gas (Fig. 3(b)). Although the thicker film always brings about poor response and recovery properties due to the longer gas diffusion path, the existence of HITP in the framework shows more profoundly accelerating effects than thickness. Experimentally, the response time (t_{res}) and recovery time (t_{rec}) are significantly reduced to < 1 min and < 10 min, respectively, when the doped HITP is 1.0 mol% or higher, which is satisfied compared with the reported chemiresistors working at room/low temperature [5, 20-23, 45, 46]. Responseconcentration log-log plots show good linearity for all sensors, based on which the detection limit of each sensor can be deduced to be 0.024–0.096 ppm (trace-level) by setting response = 10% (Fig. 3(c)) [35, 47, 48].

Figure 3(d) shows the responses of x mol% HITP doped Cu-HHTP-10C (x=0.1, 0.5, 1.0, 5.0, 10.0) toward 100 ppm NH₃ and benzene (3 sensors for each molar ratio), respectively. Both a remarkably decreased response to NH₃, from ~ 240% to ~ 80%, and a narrowly changed response to benzene between 75% and 90% can be observed. The selectivity ($S=R_{\rm benzene}/R_{\rm NH3}$) of HITP doped Cu-HHTP-10C towards benzene and NH₃ was gradually improved by increased doping amounts of HITP ligands into Cu-HHTP frameworks. An improvement in S up to ~ 220% was obtained by 10.0 mol% HITP doped Cu-HHTP-10C, of which the sensitivity toward NH₃ and benzene is reversed.

To further investigate the modulated sensitivity and selectivity of HITP doped Cu-HHTP-10C, they were studied in discriminating amongst eight typical human breath biomarkers and common interfering gases (NH3, triethylamine (TEA, N(Et)₃), methane, benzene, ethylbenzene, hydrogen, butanone, and acetone). The responses of x mol% HITP doped Cu-HHTP-10C (x = 0.1, 0.5, 1.0, 5.0, 10.0) to these gases are summarized in Fig. 3(e). Similar to NH₃, HITP doping merely results in poor sensing responses toward hydrogen, butanone, ethylbenzene and acetone. Conversely, enhanced responses were observed for alkanes and TEA. As for selectivity of gases vs. NH₃ ($S = R_{gas}/R_{NH3}$), while there are improvements for all gases with sensors of 1.0 mol% HITP dopants or higher, both reduction and enhancement can be found for those with low HITP dopants, which can be attributed to the competitive sensing activity contribution of two different coordinated metal-ligands (Fig. 3(f)). Notably, for TEA, a molecule constructed by replacing three -H of NH3 with -CH2CH3, all sensors (0.1 mol%-10.0 mol% HITP) show enhanced selectivity

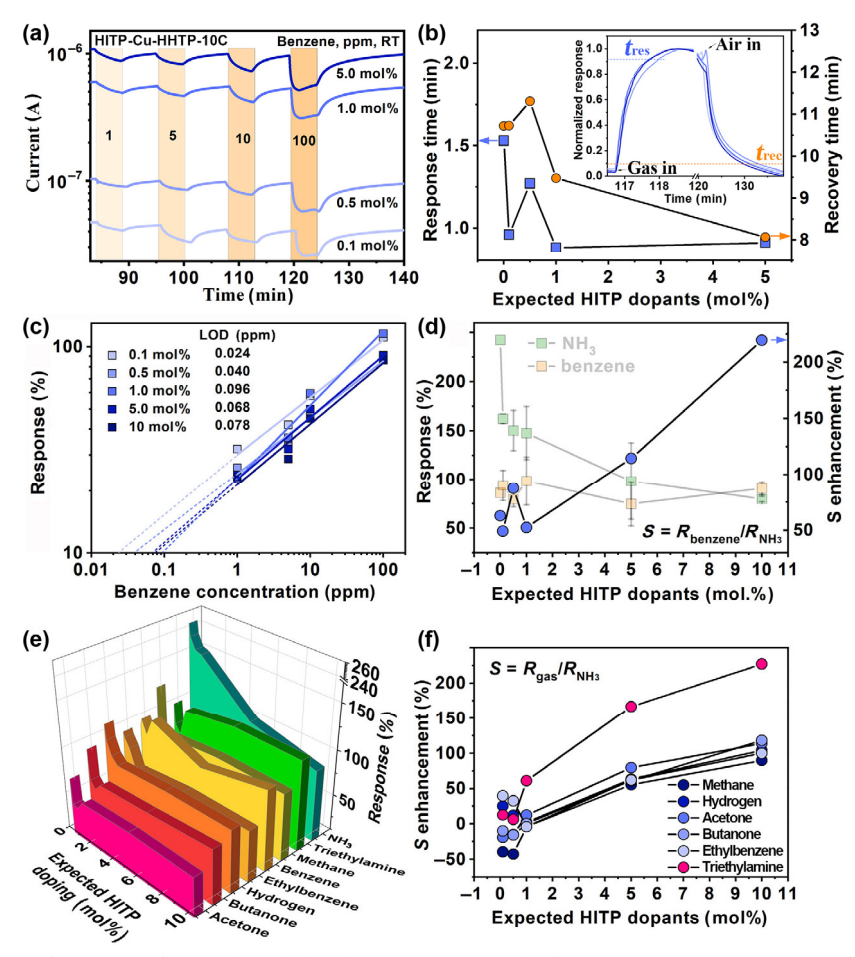


Figure 3 RT gas sensing performances of HITP ligand doped Cu-HHTP-10C: (a) the response–recovery curves toward benzene with different concentrations, (b) response–recovery time comparison to 100 ppm benzene gas (the inset is the normalized curves to 100 ppm benzene), (c) response–recovery time curves to 100 ppm NH₃ response–concentration log–log plots, (d) HITP ligand doping dependent responses comparison and selectivity improvements toward benzene and NH₃ gases, (e) the three-dimensional (3D) wall chart of responses toward different reducing gases, and (f) selectivity improvements toward triethylamine, methane, hydrogen, acetone, butanone, and ethylbenzene against NH₃.

vs. NH₃. The highest improvement in S of up to $\sim 227\%$ (10.0 mol% HITP) is similar to benzene gas and far better than other gases ($\sim 100\%$ S improvement), which may be the result of the doping induced differences on the gaseous analyte-sensing material interactions and the efficiency of charge transfer.

It is difficult to reveal the exact mechanism for the sensing performances of Cu-HHTP/HITP, HITP doped Cu-HHTP or other EC-MOFs. Experimentally, ultraviolet photoelectron spectroscopy (UPS) measurements of the EC-MOFs thin film show the up-shift of Fermi level (n-type doping effects) with the increment of HITP dopants (Figs. 4(a) and 4(b)). Despite of the shifts of Fermi level, all thin films on Au electrodes (work function, $\sim 5.1~{\rm eV}$) showed good ohmic contacts (Fig. S8 in the ESM). From the simple viewpoints of charge transfer and the resistance baseline, the n-type doping effects and reduced

resistance are in fact not good. For instance, there is lower sensitivity to smaller charge transfers upon exposure to low concentration reducing gas adsorption, which explains the reason for continuously reduced responses of sensors toward NH₃ with increased HITP dopants. Interestingly, the rich defects in thin films with HITP dopants of 1.0 mol%–10.0 mol% might be conducive to charge transfer of the framework with benzene and TEA, resulting in good sensing responses and consequently selectivity improvement over 220%.

3 Conclusions

In summary, a new dual-ligand design strategy to modulate the performance of the EC-MOF thin film was reported for the RT chemiresistive gas sensor. With a spray LbL assembly

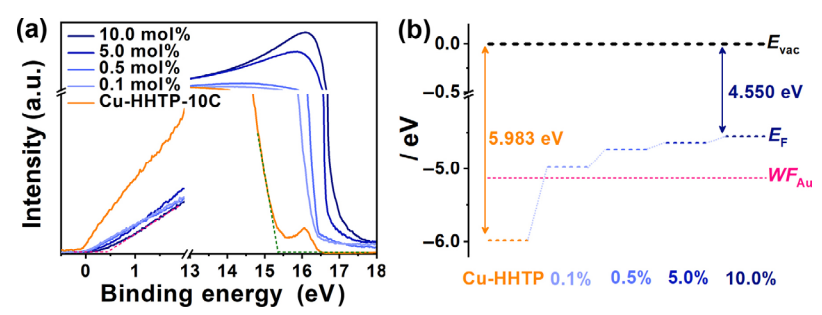


Figure 4 (a) UPS results and the corresponding (b) calculated band alignments for HITP doped Cu-HHTP-10C thin films.

method, two redox-active ligands with different coordination groups were utilized to prepare the hexagonal HITP doped Cu-HHTP-10C nanofilm. The thin film not only can be precisely prepared in nanometer scale (20–70 nm), but also shows pin hole free smooth surface. Besides, the sensitivity and selectivity of the HITP doped Cu-HHTP-10C nanofilm toward NH₃ and benzene were found to be well controlled. Selectivity improvement over 220% was realized for benzene vs. NH₃ due to rich defects caused by HITP doping. Moreover, enhanced sensing response and recovery properties were also realized by proper doping of HITP. These results indicate the potential application of the RT MOF sensor for highly sensitive and selective real-time monitoring and timely alarming of a broad range of toxic, explosive or flammable gases.

Acknowledgements

This research was supported by the National Natural Science Foundation of China (Nos. 21801243, 21822109, 21975254, 21773245, 21850410462, and 21805276), the Key Research Program of Frontier Science, CAS (No. QYZDB-SSW-SLH023), China Postdoctoral Science Foundation (Nos. 2018M642576 and 2018M642578), International Partnership Program of CAS (No. 121835KYSB201800), the Natural Science Foundation of Fujian Province (No. 2019J01129), and the Youth Innovation Promotion Association CAS.

Electronic Supplementary Material: Supplementary material (the detail characterizations include AFM, SEM, UV–Vis spectra and *I–V* measurements) is available in the online version of this article at https://doi.org/10.1007/s12274-020-2823-8.

References

- [1] Kambe, T.; Sakamoto, R.; Hoshiko, K.; Takada, K.; Miyachi, M.; Ryu, J. H.; Sasaki, S.; Kim, J.; Nakazato, K.; Takata, M. et al. π-conjugated nickel bis(dithiolene) complex nanosheet. J. Am. Chem. Soc. 2013, 135, 2462–2465.
- [2] Clough, A. J.; Skelton, J. M.; Downes, C. A.; De La Rosa, A. A.; Yoo, J. W.; Walsh, A.; Melot, B. C.; Marinescu, S. C. Metallic conductivity in a two-dimensional cobalt dithiolene metal-organic framework. J. Am. Chem. Soc. 2017, 139, 10863–10867.
- [3] Koo, W. T.; Jang, J. S.; Kim, I. D. Metal-organic frameworks for chemiresistive sensors. *Chem* 2019, 5, 1938–1963.
- [4] Dong, R. H.; Han, P.; Arora, H.; Ballabio, M.; Karakus, M.; Zhang, Z.; Shekhar, C.; Adler, P.; Petkov, P. S.; Erbe, A. et al. High-mobility band-like charge transport in a semiconducting two-dimensional metal-organic framework. *Nat. Mater.* 2018, 17, 1027–1032.
- [5] Yao, M. S.; Zheng, J. J.; Wu, A. Q.; Xu, G.; Nagarkar, S. S.; Zhang, G.; Tsujimoto, M.; Sakaki, S.; Horike, S.; Otake, K. et al. A dual-ligand porous coordination polymer chemiresistor with modulated conductivity and porosity. *Angew. Chem., Int. Ed.* 2020, 59, 172–176.
- [6] Hmadeh, M.; Lu, Z.; Liu, Z.; Gándara, F.; Furukawa, H.; Wan, S.; Augustyn, V.; Chang, R.; Liao, L.; Zhou, F. et al. New porous crystals of extended metal-catecholates. *Chem. Mater.* 2012, 24, 3511–3513.
- [7] Huang, X.; Sheng, P.; Tu, Z. Y.; Zhang, F. J.; Wang, J. H.; Geng, H.; Zou, Y.; Di, C. A.; Yi, Y. P.; Sun, Y. M. et al. A two-dimensional π-d conjugated coordination polymer with extremely high electrical conductivity and ambipolar transport behaviour. *Nat. Commun.* 2015, 6, 7408.
- [8] Takaishi, S.; Hosoda, M.; Kajiwara, T.; Miyasaka, H.; Yamashita, M.; Nakanishi, Y.; Kitagawa, Y.; Yamaguchi, K.; Kobayashi, A.; Kitagawa, H. Electroconductive porous coordination polymer Cu[Cu(pdt)₂] composed of donor and acceptor building units. *Inorg. Chem.* 2009, 48, 9048–9050.
- [9] Erickson, K. J.; Léonard, F.; Stavila, V.; Foster, M. E.; Spataru, C. D.; Jones, R. E.; Foley, B. M.; Hopkins, P. E.; Allendorf, M. D.; Talin, A. A. Thin film thermoelectric metal-organic framework with high seebeck coefficient and low thermal conductivity. Adv. Mater.

- 2015, 27, 3453-3459.
- [10] Park, S. S.; Hontz, E. R.; Sun, L.; Hendon, C. H.; Walsh, A.; Van Voorhis, T.; Dinca, M. Cation-dependent intrinsic electrical conductivity in isostructural tetrathiafulvalene-based microporous metal-organic frameworks. J. Am. Chem. Soc. 2015, 137, 1774–1777.
- [11] Darago, L. E.; Aubrey, M. L.; Yu, C. J.; Gonzalez, M. I.; Long, J. R. Electronic conductivity, ferrimagnetic ordering, and reductive insertion mediated by organic mixed-valence in a ferric semiquinoid metalorganic framework. J. Am. Chem. Soc. 2015, 137, 15703–15711.
- [12] Dong, R. H.; Zhang, Z. T.; Tranca, D. C.; Zhou, S. Q.; Wang, M. C.; Adler, P.; Liao, Z. Q.; Liu, F.; Sun, Y.; Shi, W. J. et al. A coronene-based semiconducting two-dimensional metal-organic framework with ferromagnetic behavior. *Nat. Commun.* 2018, 9, 2637.
- [13] Ko, M.; Mendecki, L.; Mirica, K. A. Conductive two-dimensional metal-organic frameworks as multifunctional materials. *Chem. Commun.* 2018, 54, 7873–7891.
- [14] Dong, R. H.; Zhang, T.; Feng, X. L. Interface-assisted synthesis of 2D materials: Trend and challenges. *Chem. Rev.* 2018, 118, 6189–6235.
- [15] Miner, E. M.; Fukushima, T.; Sheberla, D.; Sun, L.; Surendranath, Y.; Dincă, M. Electrochemical oxygen reduction catalysed by Ni₃(hexaiminotriphenylene)₂. Nat. Commun. 2016, 7, 10942.
- [16] Sheberla, D.; Bachman, J. C.; Elias, J. S.; Sun, C. J.; Shao-Horn, Y.; Dincă, M. Conductive MOF electrodes for stable supercapacitors with high areal capacitance. *Nat. Mater.* 2017, 16, 220–224.
- [17] Feng, D. W.; Lei, T.; Lukatskaya, M. R.; Park, J.; Huang, Z. H.; Lee, M.; Shaw, L.; Chen, S. C.; Yakovenko, A. A.; Kulkarni, A. et al. Robust and conductive two-dimensional metal-organic frameworks with exceptionally high volumetric and areal capacitance. *Nat. Energy* 2018. 3, 30–36.
- [18] Su, J.; He, W.; Li, X. M.; Sun, L.; Wang, H. Y.; Lan, Y. Q.; Ding, M. N.; Zuo, J. L. High electrical conductivity in a 2D MOF with intrinsic superprotonic conduction and interfacial pseudo-capacitance. *Matter* 2020, 2, 711–722.
- [19] Wu, J.; Chen, J. H.; Wang, C.; Zhou, Y.; Ba, K.; Xu, H.; Bao, W. Z.; Xu, X. H.; Carlsson, A.; Lazar, S. et al. Metal-organic framework for transparent electronics. Adv. Sci. 2020, 7, 1903003.
- [20] Yao, M. S.; Lv, X. J.; Fu, Z. H.; Li, W. H.; Deng, W. H.; Wu, G. D.; Xu, G. Layer-by-layer assembled conductive metal-organic framework nanofilms for room-temperature chemiresistive sensing. *Angew. Chem., Int. Ed.* 2017, 56, 16510–16514.
- [21] Campbell, M. G.; Sheberla, D.; Liu, S. F.; Swager, T. M.; Dincă, M. Cu₃(hexaiminotriphenylene)₂: An electrically conductive 2D metalorganic framework for chemiresistive sensing. *Angew. Chem., Int. Ed.* 2015, 127, 4423–4426.
- [22] Yao, M. S.; Xiu, J. W.; Huang, Q. Q.; Li, W. H.; Wu, W. W.; Wu, A. Q.; Cao, L. A.; Deng, W. H.; Wang, G. E.; Xu, G. Van der waals heterostructured MOF-on-MOF thin films: Cascading functionality to realize advanced chemiresistive sensing. *Angew. Chem., Int. Ed.* 2019, 58, 14915–14919.
- [23] Meng, Z.; Aykanat, A.; Mirica, K. A. Welding metallophthalocyanines into bimetallic molecular meshes for ultrasensitive, low-power chemiresistive detection of gases. J. Am. Chem. Soc. 2018, 141, 2046–2053.
- [24] Wu, G. D.; Huang, J. H.; Zang, Y.; He, J.; Xu, G. Porous field-effect transistors based on a semiconductive metal-organic framework. J. Am. Chem. Soc. 2016, 139, 1360–1363.
- [25] Mu, Q. Q.; Zhu, W.; Li, X.; Zhang, C. F.; Su, Y. H.; Lian, Y. B.; Qi, P. W.; Deng, Z.; Zhang, D.; Wang, S. et al. Electrostatic charge transfer for boosting the photocatalytic CO₂ reduction on metal centers of 2D MOF/rGO heterostructure. *Appl. Catal. B Environ*. 2020, 262, 118144.
- [26] Xu, C. Y.; Pan, Y. T.; Wan, G.; Liu, H.; Wang, L.; Zhou, H.; Yu, S. H.; Jiang, H. L. Turning on visible-light photocatalytic C-H oxidation over metal-organic frameworks by introducing metal-to-cluster charge transfer. J. Am. Chem. Soc. 2019, 141, 19110–19117.
- [27] Jiang, H. Q.; Liu, X. C.; Wu, Y. S.; Shu, Y. F.; Gong, X.; Ke, F. S.; Deng, H. X. Metal-organic frameworks for high charge-discharge rates in lithium-sulfur batteries. *Angew. Chem., Int. Ed.* 2018, 57, 3916–3921.
- [28] Meng, Z.; Stolz, R. M.; Mendecki, L.; Mirica, K. A. Electricallytransduced chemical sensors based on two-dimensional nanomaterials.

6 Nano Res.

- Chem. Rev. 2019, 119, 478-598.
- [29] Sun, L.; Campbell, M. G.; Dincă, M. Electrically conductive porous metal-organic frameworks. *Angew. Chem., Int. Ed.* 2016, 55, 3566– 3579.
- [30] Choi, S. J.; Kim, I. D. Recent developments in 2D nanomaterials for chemiresistive-type gas sensors. *Electron. Mater. Lett.* 2018, 14, 221–260.
- [31] Campbell, M. G.; Dincă, M. Metal-organic frameworks as active materials in electronic sensor devices. Sensors 2017, 17, 1108.
- [32] Guo, L. L.; Chen, F.; Xie, N.; Kou, X. Y.; Wang, C.; Sun, Y. F.; Liu, F. M.; Liang, X. S.; Gao, Y.; Yan, X. et al. Ultra-sensitive sensing platform based on Pt-ZnO-In₂O₃ nanofibers for detection of acetone. Sens. Actuators B Chem. 2018, 272, 185–194.
- [33] Liu, H.; Li, M.; Voznyy, O.; Hu, L.; Fu, Q. Y.; Zhou, D. X.; Xia, Z.; Sargent, E. H.; Tang, J. Physically flexible, rapid-response gas sensor based on colloidal quantum dot solids. *Adv. Mater.* 2014, 26, 2718–2724.
- [34] Jian, Y. Y.; Hu, W. W.; Zhao, Z. H.; Cheng, P. F.; Haick, H.; Yao, M. S.; Wu, W. W. Gas sensors based on chemi-resistive hybrid functional nanomaterials. *Nano-Micro Lett.* 2020, 12, 71.
- [35] Yao, M. S.; Tang, W. X.; Wang, G. E.; Nath, B.; Xu, G. Mof thin film-coated metal oxide nanowire array: Significantly improved chemiresistor sensor performance. Adv. Mater. 2016, 28, 5229–5234.
- [36] Zhang, J.; Liu, X. H.; Neri, G.; Pinna, N. Nanostructured materials for room-temperature gas sensors. Adv. Mater. 2016, 28, 795–831.
- [37] Kim, H. J.; Lee, J. H. Highly sensitive and selective gas sensors using p-type oxide semiconductors: Overview. Sens. Actuators B Chem. 2014, 192, 607–627.
- [38] Li, T. M.; Zeng, W.; Wang, Z. C. Quasi-one-dimensional metal-oxide-based heterostructural gas-sensing materials: A review. Sens. Actuators B Chem. 2015, 221, 1570–1585.
- [39] Shi, Z. L.; Tao, Y.; Wu, J. S.; Zhang, C. Z.; He, H. L.; Long, L. L.; Lee, Y.; Li, T.; Zhang, Y. B. Robust metal-triazolate frameworks for

- CO₂ capture from flue gas. J. Am. Chem. Soc. 2020, 142, 2750-2754.
- [40] Heinke, L.; Wöll, C. Surface-mounted metal-organic frameworks: Crystalline and porous molecular assemblies for fundamental insights and advanced applications. Adv. Mater. 2019, 31, 1806324.
- [41] Gu, Y. F.; Wu, Y. N.; Li, L. C.; Chen, W.; Li, F. T.; Kitagawa, S. Controllable modular growth of hierarchical MOF-on-MOF architectures. *Angew. Chem., Int. Ed.* 2017, 56, 15658–15662.
- [42] Shekhah, O.; Hirai, K.; Wang, H.; Uehara, H.; Kondo, M.; Diring, S.; Zacher, D.; Fischer, R. A.; Sakata, O.; Kitagawa, S. et al. MOF-on-MOF heteroepitaxy: Perfectly oriented [Zn₂(ndc)₂(dabco)]_n grown on [Cu₂(ndc)₂(dabco)]_n thin films. *Dalton Trans.* 2011, 40, 4954–4958.
- [43] Richardson, J. J.; Björnmalm, M.; Caruso, F. Technology-driven layer-by-layer assembly of nanofilms. *Science* 2015, 348, aaa2491.
- [44] Li, W. H.; Ding, K.; Tian, H. R.; Yao, M. S.; Nath, B.; Deng, W. H.; Wang, Y. B.; Xu, G. Conductive metal-organic framework nanowire array electrodes for high-performance solid-state supercapacitors. *Adv. Funct. Mater.* 2017, 27, 1702067.
- [45] Hu, N. T.; Yang, Z.; Wang, Y. Y.; Zhang, L. L.; Wang, Y.; Huang, X. L.; Wei, H.; Wei, L. M.; Zhang, Y. F. Ultrafast and sensitive room temperature NH₃ gas sensors based on chemically reduced graphene oxide. *Nanotechnology* 2013, 25, 025502.
- [46] Chen, E. X.; Yang, H.; Zhang, J. Zeolitic imidazolate framework as formaldehyde gas sensor. *Inorg. Chem.* 2014, 53, 5411–5413.
- [47] Yao, M. S.; Li, Q. H.; Hou, G. L.; Lu, C.; Cheng, B. L.; Wu, K. C.; Xu, G; Yuan, F. L.; Ding, F.; Chen, Y. F. Dopant-controlled morphology evolution of WO₃ polyhedra synthesized by RF thermal plasma and their sensing properties. ACS Appl. Mater. Interfaces 2015, 7, 2856–2866.
- [48] Yao, M. S.; Cao, L. A.; Tang, Y. X.; Wang, G. E.; Liu, R. H.; Kumar, P. N.; Wu, G. D.; Deng, W. H.; Hong, W. J.; Xu, G. Gas transport regulation in a MO/MOF interface for enhanced selective gas detection. J. Mater. Chem. A 2019, 7, 18397–18403.